High-spin states in odd-odd ^{170}Ta

Y. H. Zhang, S. Q. Zhang, Q. Z. Zhao, S. F. Zhu, H. S. Xu, X. H. Zhou, Y. X. Guo, X. G. Lei, J. Lu, W. X. Huang, Q. B. Gou, H. J. Jin, Z. Liu, Y. X. Luo, X. F. Sun, and Y. T. Zhu
Institute of Modern Physics, the Chinese Academy of Sciences, Lanzhou 730000, People's Republic of China

X. G. Wu, S. X. Wen, and C. X. Yang
China Institute of Atomic Energy, P.O. Box 275, Beijing 102413, People's Republic of China
(Received 29 March 1999; published 9 September 1999)

High-spin states in ^{170}Ta have been studied via ^{159}Tb(^{16}O,5$n\gamma$)^{170}Ta reaction through excitation functions, K x-γ, and γ-γ-t coincidence measurements. Three rotational bands have been identified which consist of two strongly coupled bands and a semidecoupled one. The quasiparticle configurations of these bands and the interpretation of experimental results are discussed based on the existing knowledge of neighboring odd-mass and odd-odd nuclei and in the framework of the cranked-shell model. Low-spin signature inversion in the $\pi 9/2^-[514]\otimes\nu 5/2^+[642]$ and $\pi 1/2^-[541]\otimes\nu 5/2^+[642]$ bands are discussed. A delay (reduction) of the band-crossing frequency is observed in the $\pi 1/2^-[541]\otimes\nu 5/2^+[642]$ ($\pi 5/2^+[402]\otimes\nu 5/2^+[642]$) band. This configuration-dependent crossing frequency is discussed in comparison with the *AB* crossing frequencies in the related bands of neighboring odd-Z isotopes. [S0556-2813(99)04809-8]

PACS number(s): 21.10.Re, 23.20.Lv, 27.70.+q

I. INTRODUCTION

The high-spin states of deformed odd-odd nuclei are normally difficult for spectroscopic studies because of high level density at low excitation energies. In spite of this, more and more experimental data have been accumulated concerning the band structures of odd-odd nuclei in the rare-earth region. The well-known anomalous signature splitting (so-called low-spin signature inversion in energy) at low rotational frequencies has been systematically found and confirmed in the $\pi h_{11/2}\otimes\nu i_{13/2}$ bands of ^{152}Eu [1], ^{154,156}Tb [2], $^{156-160}$Ho [3–9], $^{158-166}$Tm [10–21], $^{160-166}$Lu [22–31], and ^{166,168}Ta [31–33] nuclei, respectively. This striking feature has been extensively studied through various theoretical approaches, such as the cranked-shell model [34,35], the particle rotor model [36–38], the projected shell model [39,40], and the interacting boson-fermion model [41], respectively. Recently the low-spin signature inversion has also been observed in the $\pi 7/2^+[404]\otimes\nu 5/2^+[642]$ band of ^{166}Tm [20] and in the $\pi 1/2^-[541]\otimes\nu i_{13/2}$ semidecoupled bands of ^{162,164}Tm and ^{174}Ta [42]. Another interesting phenomenon is the anomalous large band crossing frequencies observed in the $\pi h_{11/2}\otimes\nu h_{9/2}$ bands of ^{160}Tm [16] and ^{164}Lu [28,29], and in the $\pi h_{9/2}\otimes\nu p_{3/2}$ band of ^{170}Lu [43]. This anomaly has been regarded as the partial disappearance of the odd neutron blocking effect and attributed, tentatively, to the unknown residual proton-neutron interactions [29,43]. Since only a few cases have been observed, one may ask if these anomalies could be found in a wide nuclear region or in the bands with other quasiparticle configurations. The answer to this question calls for systematic and further experimental investigations. ^{170}Ta seems to be a good candidate for further studies so long as its location in the chart of nuclides is concerned. Prior to this work, the high-spin states of ^{170}Ta were less extensively studied [44]. In order to get more information about the band structures of ^{170}Ta, further investigations have been carried out by using the in-beam γ-spectroscopy techniques. Preliminary reports of this work have been published elsewhere [45,46], the more detailed results are presented in this paper.

II. EXPERIMENTAL METHODS AND RESULTS

The high-spin states of ^{170}Ta were populated through ^{159}Tb(^{16}O,5$n\gamma$) fusion-evaporation reaction at 105 MeV beam energy. The target consisted of a 2 mg/cm^2 ^{159}Tb metallic foil with 3 mg/cm^2 Pb backing. The beam was provided by the sector focusing cyclotron in the Heavy Ion Research Facility Lanzhou (HIRFL). The in-beam γ rays were detected by using four high-purity germanium detectors with BGO anti-Compton shields placed at $\pm 90°$, $30°$, and $145°$ with respect to the beam direction, respectively. In order to search for the possible isomeric states, the time window Δt of 600 ns was set in the coincidence measurement. A total of 80×10^6 γ_1-γ_2-$t_{\gamma_1\gamma_2}$ events were accumulated in this experiment. Preliminary data analysis showed that at least three rotational bands could be assigned to ^{170}Ta. To confirm this assignment, the excitation functions and K x-γ coincidence measurement were performed in the HI-13 tandem accelerator of China Institute of Atomic Energy (CIAE) using the same reaction as in HIRFL. The beam energy was varied from 85 to 102 MeV and the 18-elements BGO multiplicity filter [47] was used which subtends 70% solid angles of the up-hemisphere around the target. The singles γ spectrum in this experiment was very complicated; many γ rays coming from the in-beam products of ^{169,170,171}Ta [48,44], ^{169,170}Hf [49,50], and ^{167}Lu [51] were observed together with their corresponding residual radioactivities. To enhance the in-beam cascade γ rays, at least a fourfold requirement of this BGO array has been imposed during the excitation function measurements. The excitation functions for some uncontaminated γ rays have been obtained and shown in Fig. 1, from which the γ rays of ^{170}Ta ($5n$ channel) and ^{170}Hf ($p4n$

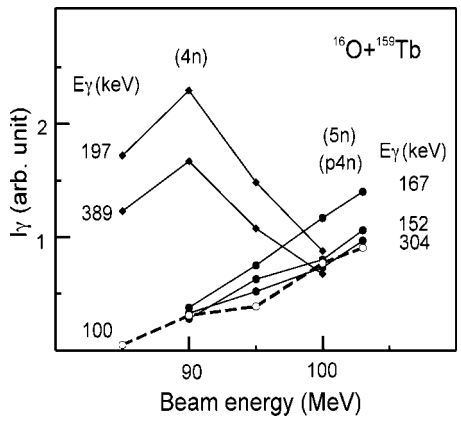

FIG. 1. Excitation functions for some uncontaminated γ rays.

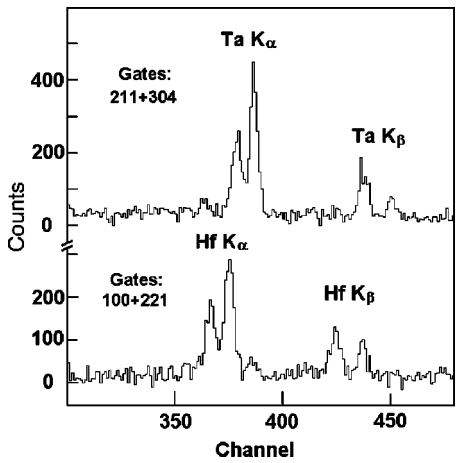

FIG. 2. Spectra measured in x-ray detector in coincidence with γ rays in HPGe.

channel) can been clearly separated from that of ^{171}Ta ($4n$ channel).

The K x-γ coincidence measurement was carried out at 100 MeV beam energy by using one planar detector and seven high-purity germanium detectors with BGO anti-Compton shields. About 4.5 million K x-γ and 33 million γ-γ coincidence events were accumulated. In both experiments, the detectors were calibrated by the standard ^{152}Eu, ^{133}Ba, and ^{60}Co sources and also checked by the known in-beam γ rays of ^{169}Ta [48] and ^{170}Hf [49]. The typical energy resolutions were about 2.0–2.4 keV at full width at half maximum for the 1332.5 keV line. The time resolution was about 12 ns for the in-beam prompt γ-γ cascade. The detection efficiency was calibrated by using standard ^{133}Ba and ^{152}Eu sources.

After the gain matching of the detectors, four $4k\times4k$ matrices have been constructed at different time conditions, including a prompt γ-γ matrix (-36 ns$\leqslant t_{\gamma_1\gamma_2}\leqslant+36$ ns), a delayed γ-γ matrix ($+12$ ns$\leqslant t_{\gamma_1\gamma_2}\leqslant+600$ ns), a pre-prompt γ-γ matrix (-600 ns$\leqslant t_{\gamma_1\gamma_2}\leqslant-12$ ns) and a prompt x-γ matrix (-40 ns$\leqslant t_{\gamma_1\gamma_2}\leqslant+40$ ns). Figure 2 shows the low-energy coincidence spectrum gated by some uncontaminated γ rays recorded in the HPGe detectors; the K x rays from Ta and Hf isotopes are firmly distinguished. From excitation functions and K x-γ coincidence measurement, some typical γ rays and thus the associated rotational bands can be firmly attributed to ^{170}Ta.

The level scheme of ^{170}Ta deduced from present work is shown in Fig. 3 which consists of three rotational bands labeled as A, B, and C. Three bands are floating in energy since the connection of the bandheads with the ground state or

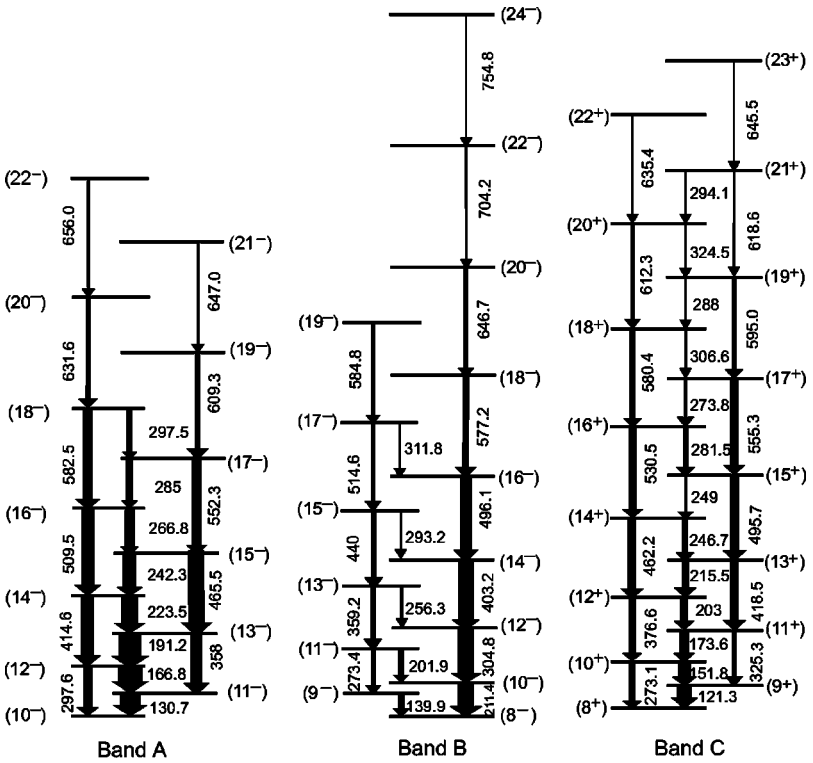

FIG. 3. Partial level scheme of ^{170}Ta deduced from the present work.

low-lying levels [52,53] has not been established. The ordering of transitions in various bands is mainly based on the γ ray relative intensities, γ-γ coincidence relationships and γ ray energy sums. The sum-gates coincidence spectra for bands *A*, *B*, and *C* are given in Figs. 4(a)–4(c) where the γ lines belonging to these bands are clearly shown. The γ ray energies, spin-parity assignments, relative γ-ray intensities, branching ratios, extracted $B(M1)/B(E2)$ ratios, and their placement in the level scheme are presented in Table I grouped in sequences for each band.

The spins of energy levels are proposed on the basis of the additivity rule for alignments i_x (configuration assignment to bands *A*, *B*, and *C* will be discussed in the next section). Figures 5(a)–5(c) depict the quasiparticle alignments for the three bands in ^{170}Ta and the associated one-quasiparticle bands in ^{169}Ta and ^{169}Hf. It is shown that this simple additivity property for alignments is well satisfied at lower frequencies using the proposed spin values. For example, the alignments for $\pi 9/2^-[514]$ and $\nu 5/2^+[642]$ bands at $\hbar\omega = 0.2$ MeV are $1.8\hbar$ and $4.1\hbar$, respectively, the experimental alignment of $\pi 9/2^-[514] \otimes \nu 5/2^+[642]$ band (band *A*) in ^{170}Ta is $5.8\hbar$, very close to the predicted value of $5.9\hbar$. It should be noted that the Harris parameters used as a reference have certain influences on the extracted alignment and thus on the spin assignment. In our calculations, these parameters are considered to be configuration dependent. Using the method proposed and applied in Refs. [13,16,17], the Harris parameters J_0 and J_1 have been extracted and presented in Table II by fitting the local moment of the inertia of each band at lower rotational frequencies before the first band crossing.

An additional argument for the spin assignment of band *A* comes from the systematics of level spacings in the similar bands of lighter Ta isotopes. The relative excitation energies, normalized to the (12^-) level, are presented in Fig. 6 for the favored (signature $\alpha = 0$) $\Delta I = 2$ transition sequences in the $\pi h_{11/2} \otimes \nu i_{13/2}$ bands of $^{158-166}$Tm, $^{160-166}$Lu, and $^{166-170}$Ta nuclei. As is clear from this figure, the level energies of these bands exhibit smooth trends for a set of isotopes indicating a smooth variation of nuclear deformation with neutron number. The level energies of band *A* in ^{170}Ta fit well with the systematics if the proposed I^π values are accepted. The criterion of energy systematics is also applied in band *B* as shown in Fig. 7, where the relative excitation energies, normalized to the (10^-) level, are compared with each other between the semidecoupled bands in $^{170-176}$Ta, ^{168}Lu, and ^{162,164}Tm. Note that the firm spin assignments have been made for ^{174}Ta and ^{162,164}Tm [42], respectively. The data for ^{168}Lu and ^{176}Ta are taken from [54,55]. The I^π values for ^{172}Ta are increased arbitrarily by $3\hbar$ with respect to the original assignment [56] in line with the suggestion in [57]. Relying on the systematics of level spacings, the lowest level in band *B* could be proposed as $I_0 = (8^-)$, which is $1\hbar$ increased comparing with our previous suggestion [45,46]. As limited by the method used here, an uncertainty within $2\hbar$ may be introduced to the present spin assignment shown in Fig. 3.

For the three rotational bands shown in Fig. 3, branching ratios defined as

$$\lambda = \frac{T_\gamma(I \to I-2)}{T_\gamma(I \to I-1)} \tag{1}$$

were extracted for most of the transitions. Here $T_\gamma(I \to I-2)$ and $T_\gamma(I \to I-1)$ are the γ-ray intensities of the $\Delta I = 2$ and $\Delta I = 1$ transitions, respectively. These intensities were measured in a summed coincidence spectrum gated by the transitions above the state of interest. The branching ratios were used to extract relative transition probabilities defined as

$$\frac{B(M1, I \to I-1)}{B(E2, I \to I-2)} = 0.697 \frac{[E_\gamma(I \to I-2)]^5}{[E_\gamma(I \to I-1)]^3} \frac{1}{\lambda} \frac{1}{1+\delta^2}, \tag{2}$$

where δ is the $E2/M1$ mixing ratio for the $\Delta I = 1$ transitions, $E_\gamma(I \to I-1)$ and $E_\gamma(I \to I-2)$ are the $\Delta I = 2$ and $\Delta I = 1$ transition energies, respectively. Because of the complexity of related γ rays and the poor statistics of our data, no mixing ratios could be deduced, therefore δ has been set to zero in the calculations. The error introduced under this assumption is expected to be small, since mixing ratios measured for neighboring ^{171}Ta [44], ^{176}Re [57], and ^{166}Tm [19] nuclei have been shown to be small. The extracted $B(M1, I \to I-1)/B(E2, I \to I-2)$ ratios are presented as a function of spin in Fig. 8. These ratios are also tabulated in Table I.

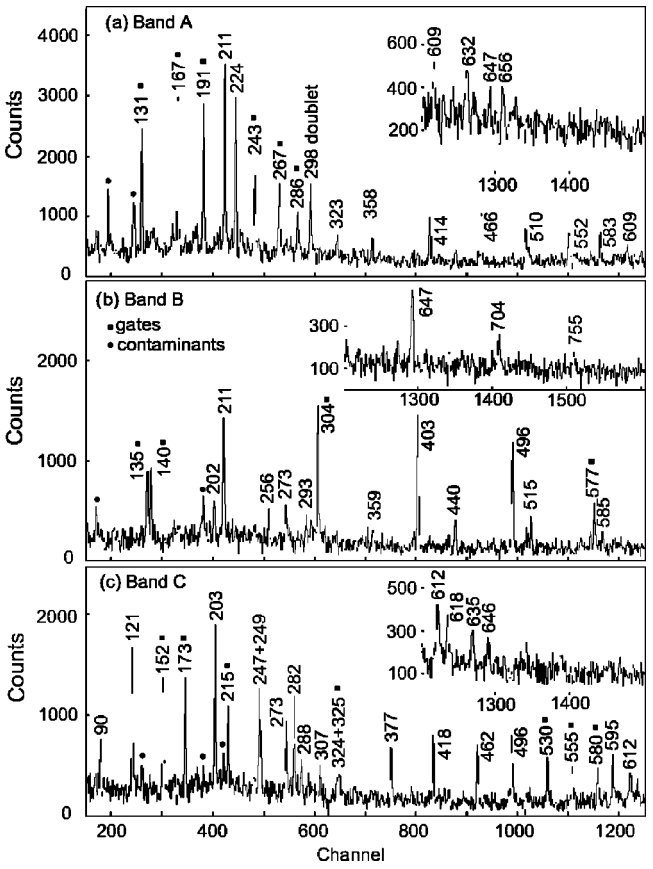

FIG. 4. γ ray coincidence spectra corresponding to the sum gates (as indicated in the figures) for three bands *A*, *B*, and *C*. The peaks labeled (●) are contaminants.

TABLE I. γ-ray transition energies, spin assignment, γ intensities, branching ratios, and extracted $B(M1)/B(E2)$ ratios in ^{170}Ta.

E_γ(keV)[a]	$J_i^\pi \rightarrow J_f^\pi$ [b]	I_γ [c]	λ [d]	$B(M1)/B(E2)$ [e] (μ_N^2/e^2b^2)	Multipolarity
Band *A*					
211 [f]		95.7			
130.7	$(11^-)\rightarrow(10^-)$	84.3			$(M1/E2)$
297.6	$(12^-)\rightarrow(10^-)$	35.4	0.235	1.49	$(E2)$
166.8	$(12^-)\rightarrow(11^-)$	100			$(M1/E2)$
358	$(13^-)\rightarrow(11^-)$	46.8	0.468	1.25	$(E2)$
191.2	$(13^-)\rightarrow(12^-)$	94.3			$(M1/E2)$
414.6	$(14^-)\rightarrow(12^-)$	53.4	0.833	0.918	$(E2)$
223.5	$(14^-)\rightarrow(13^-)$	66.1			$(M1/E2)$
465.5	$(15^-)\rightarrow(13^-)$	64.9	0.96	1.12	$(E2)$
242.3	$(15^-)\rightarrow(14^-)$	55.5			$(M1/E2)$
509.5	$(16^-)\rightarrow(14^-)$	52.0	1.35	0.92	$(E2)$
266.8	$(16^-)\rightarrow(15^-)$	38.3			$(M1/E2)$
552.3	$(17^-)\rightarrow(15^-)$	38.0	1.5	1.02	$(E2)$
285	$(17^-)\rightarrow(16^-)$	25.3			$(M1/E2)$
582.5	$(18^-)\rightarrow(16^-)$	39.6	1.84	0.965	$(E2)$
297.5	$(18^-)\rightarrow(17^-)$	20.0			$(M1/E2)$
609.3	$(19^-)\rightarrow(17^-)$	20.4			$(E2)$
631.6	$(20^-)\rightarrow(18^-)$	18.1			$(E2)$
647.0	$(21^-)\rightarrow(19^-)$	$\leqslant$10			$(E2)$
656.0	$(22^-)\rightarrow(20^-)$	$\leqslant$10			$(E2)$
Band *B*					
135 [f]		41.0			
139.9	$(9^-)\rightarrow(8^-)$	23.8			$(M1/E2)$
211.4	$(10^-)\rightarrow(8^-)$	67.5			$(E2)$
273.5	$(11^-)\rightarrow(9^-)$	15.9	0.853	0.152	$(E2)$
201.9	$(11^-)\rightarrow(10^-)$	20.5			$(M1/E2)$
304.8	$(12^-)\rightarrow(10^-)$	63.9			$(E2)$
359.2	$(13^-)\rightarrow(11^-)$	18.4	2.08	0.119	$(E2)$
256.3	$(13^-)\rightarrow(12^-)$	10.2			$(M1/E2)$
403.2	$(14^-)\rightarrow(12^-)$	59.4			$(E2)$
440.0	$(15^-)\rightarrow(13^-)$	20.4	1.449	0.315	$(E2)$
293.2	$(15^-)\rightarrow(14^-)$	6.5			$(M1/E2)$
496.1	$(16^-)\rightarrow(14^-)$	44.8			$(E2)$
514.6	$(17^-)\rightarrow(15^-)$	14.3	3.76	0.221	$(E2)$
311.8	$(17^-)\rightarrow(16^-)$	3.8			$(M1/E2)$
577.2	$(18^-)\rightarrow(16^-)$	26.1			$(E2)$
584.8	$(19^-)\rightarrow(17^-)$	10.9			$(E2)$
646.7	$(20^-)\rightarrow(18^-)$	14.7			$(E2)$
704.2	$(22^-)\rightarrow(20^-)$	6.6			$(E2)$
754.8	$(24^-)\rightarrow(22^-)$	$\leqslant$5			$(E2)$
Band *C*					
90 [f]		30.5			
121.3	$(9^+)\rightarrow(8^+)$	59.4			$(M1/E2)$
273.1	$(10^+)\rightarrow(8^+)$	25.1	0.527	0.574	$(E2)$
151.8	$(10^+)\rightarrow(9^+)$	52.9			$(M1/E2)$
325.3	$(11^+)\rightarrow(9^+)$	17.7	0.761	0.637	$(E2)$
173.6	$(11^+)\rightarrow(10^+)$	37.3			$(M1/E2)$
376.6	$(12^+)\rightarrow(10^+)$	25.8	1.263	0.50	$(E2)$
203.0	$(12^+)\rightarrow(11^+)$	27.9			$(M1/E2)$

TABLE I. (*Continued.*)

E_γ(keV)[a]	$J_i^\pi \rightarrow J_f^\pi$ [b]	I_γ [c]	λ [d]	$B(M1)/B(E2)$ [e] (μ_N^2/e^2b^2)	Multipolarity
418.5	$(13^+)\rightarrow(11^+)$	32.5	1.478	0.605	$(E2)$
215.5	$(13^+)\rightarrow(12^+)$	24.4			$(M1/E2)$
462.2	$(14^+)\rightarrow(12^+)$	31.2	1.776	0.553	$(E2)$
246.7	$(14^+)\rightarrow(13^+)$	21.4			$(M1/E2)$
495.7	$(15^+)\rightarrow(13^+)$	35.3	3.287	0.411	$(E2)$
249.0	$(15^+)\rightarrow(14^+)$	10.6			$(M1/E2)$
530.5	$(16^+)\rightarrow(14^+)$	28.0	2.08	0.64	$(E2)$
281.5	$(16^+)\rightarrow(15^+)$	18.7			$(M1/E2)$
555.3	$(17^+)\rightarrow(15^+)$	30.4	2.98	0.58	$(E2)$
273.8	$(17^+)\rightarrow(16^+)$	13.2			$(M1/E2)$
580.4	$(18^+)\rightarrow(16^+)$	22.3	3.64	0.44	$(E2)$
306.6	$(18^+)\rightarrow(17^+)$	9.9			$(M1/E2)$
595.0	$(19^+)\rightarrow(17^+)$	18.1	2.36	0.92	$(E2)$
288.0	$(19^+)\rightarrow(18^+)$	7.4			$(M1/E2)$
612.3	$(20^+)\rightarrow(18^+)$	14.3	1.75	1.0	$(E2)$
324.5	$(20^+)\rightarrow(19^+)$	7.4			$(M1/E2)$
618.6	$(21^+)\rightarrow(19^+)$	8.85	1.45	1.712	$(E2)$
294.1	$(21^+)\rightarrow(20^+)$	6.1			$(M1/E2)$
635.4	$(22^+)\rightarrow(20^+)$	7.1			$(E2)$
645.5	$(23^+)\rightarrow(21^+)$	5.1			$(E2)$

[a]Uncertainties between 0.1 and 0.3 keV.

[b]Spin assignment based on energy systematics and additivity rule of i_x.

[c]Uncertainties between 5 and 30 % keV.

[d]Branching ratio: $T_\gamma(I\rightarrow I-2)/T_\gamma(I\rightarrow I-1)$, $T_\gamma(I\rightarrow I-2)$, and $T_\gamma(I\rightarrow I-1)$ are the relative γ intensities of the $E2$ and $M1$ transition depopulating the level I, respectively.

[e]Determined assuming $\delta^2=0$.

[f]211, 135, and 90 keV lines, not placed in the level scheme, depopulate bands *A*, *B*, *C*, respectively.

The relative intensities of γ rays were extracted and tabulated in Table I. These intensities were corrected for detection efficiencies and normalized to the intensity of the 166.8 keV line ($=100$) in band *A*. Note that the relative intensities are measured in the total projection spectrum or the spectra gated on the bottom transition of the band. Such a restriction means that the errors associated with relative intensities are often larger than those associated with the branching ratios, since the latter were obtained by gating on clean transitions above each state of interest. The experimental $B(M1)/B(E2)$ ratios for the three bands are compared with the theoretical values as shown in Fig. 8. These calculations are carried out using a semiclassical formula for $B(M1)$ values derived from the geometrical model of Ref. [58]

$$B(M1,I\rightarrow I-1)=\frac{3}{8\pi}[(g_p-g_{_R})A+(g_n-g_{_R})B]^2, \quad (3)$$

$$A=\left(1-\frac{K^2}{I^2}\right)^{1/2}\Omega_p-i_p\frac{K}{I}, \quad (4)$$

$$B=\left(1-\frac{K^2}{I^2}\right)^{1/2}\Omega_n-i_n\frac{K}{I}. \quad (5)$$

Here $g_{p(n)}$, $i_{p(n)}$, and $\Omega_{p(n)}$ represent the g factor, the alignment, and the projection angular momentum component on the symmetry axis of the proton (neutron) in the associated neighboring odd-mass nuclei. These values are taken from the compilation in Refs. [8,20,59,60] and are presented in Table II. For some cases they are calculated using the method described in Refs. [59,60] if the experimental intraband branching ratio and magnetic moment [61] are available.

The values of $B(E2;I\rightarrow I-1)$ are calculated according to the expression [8]

$$B(E2,I\rightarrow I-2)=\frac{5}{16\pi}\langle IK20|I-2K\rangle^2Q_0^2. \quad (6)$$

The Q_0 is the intrinsic quadrupole moment of the nucleus, we take the average of its even-even neighbors as $Q_0=7.0(b)$. The collective g factors of odd-odd nucleus g_R in variant quasiparticle configurations are calculated using the expression [8]

$$g_R=g_R(p)+g_R(n)-g_R(e-e), \quad (7)$$

where $g_R(p)$, $g_R(n)$, and $g_R(e-e)$ represent the collective g factor of neighboring odd-*Z*, odd-*N*, and even-even nuclei,

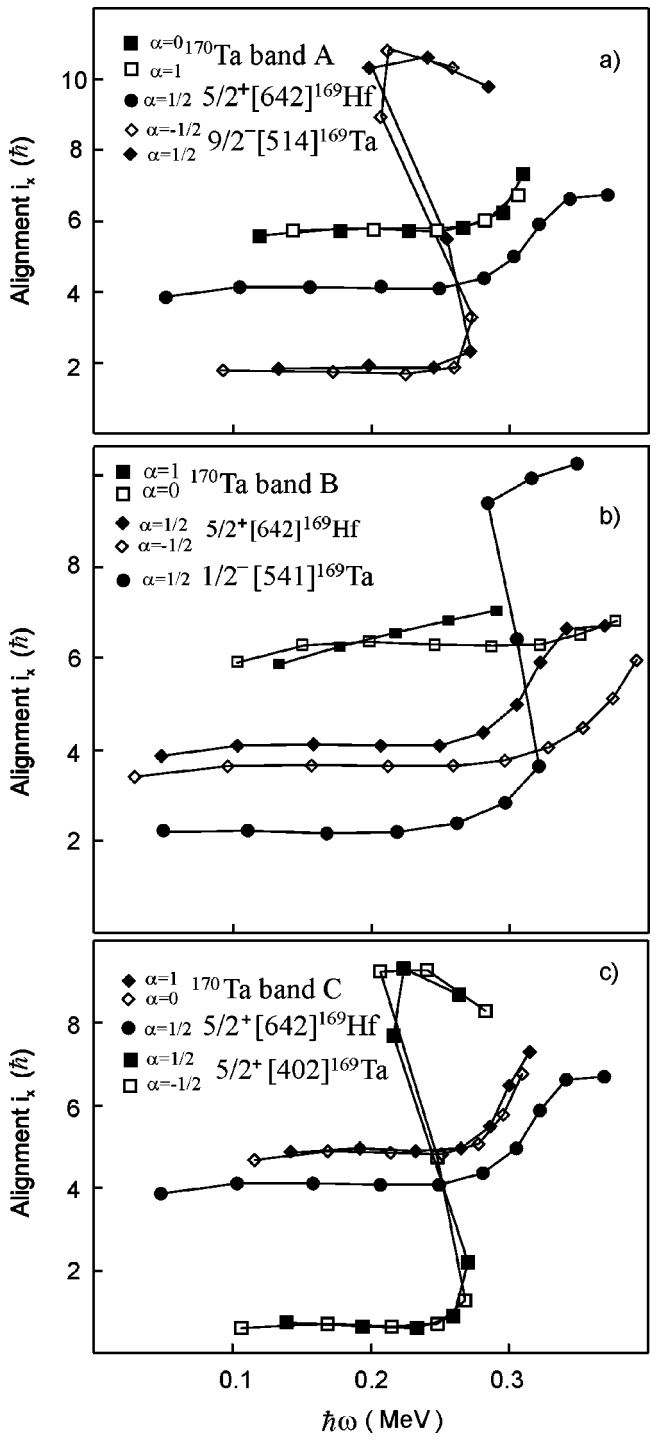

FIG. 5. Plot of alignments i_x versus frequencies $\hbar\omega$ for (a) band *A*, (b) band *B*, and (c) band *C* in ^{170}Ta and the associated one-quasiparticle bands in ^{169}Ta [48] and ^{169}Hf [49].

respectively. The average value of $g_R(e-e)=0.292$ is used in the calculation. The *K* value is the effective component of the intrinsic angular momentum onto the symmetry axis [58]. For the strongly coupled bands in an odd-odd nucleus, the *K* values are assumed to be $K_{\pm}=|\Omega_p \pm \Omega_n|$ according to Gallagher-Moszkowski coupling rules [62]. For the semide-coupled band, significant Coriolis mixing may present on account of the high-*j* parentage of both participating orbitals ($j_p=9/2$, $j_n=13/2$), and the expected *K* value may differ at higher spin from that at lower spins. In this case, two *K* values ($K=2\hbar,3\hbar$) are used in the calculations.

Great efforts have been made to search for the isomeric states in ^{170}Ta by analyzing carefully the γ_1-γ_2-$t_{\gamma_1\gamma_2}$ coincidence data. Two γ rays seem to be in delayed coincidence with the associated intraband transitions (211 keV line with band *A*, and 135 kev line with band *B*). The half-lives of the possible isomeric states have not been determined due to the poor statistics.

III. DISCUSSIONS

From the known β decay of ^{170}Ta to excited 2^+ and 4^+ states in ^{170}Hf, a 3^+ ground state of ^{170}Ta with $\pi 1/2^-[541]\otimes\nu 5/2^-[523]$ quasiparticle configuration was proposed [52,63]. The only established excited state was evaluated as $I^{\pi}=1^+$ which feeds directly to a 3^+ ground state via 316 keV γ radiation. A study of β decay of ^{170}W leads to the discovery of several low-energy γ rays [53]. All these γ rays have not been observed in our experiment. Prior to this work, the high-spin states of ^{170}Ta have been observed in Ref. [44] which, to some extent, are different from the present work. Because of the poor statistics of our data, directional correlations from oriented states ratios for the γ transitions have not been extracted, the multipolarities of stretched $E2$ characters for the crossover transitions and the $M1/E2$ intraband transitions have been assumed. In the following, some properties will be discussed concerning the signature inversion, alignments, band crossing frequencies, and transition rates, respectively.

The structure of an odd-odd nucleus is expected to be associated with that of the neighboring even-even and odd-mass nuclei. Some general properties can be found in Refs. [26,64] concerning the ground-state quadrupole deformation of even-even and odd-*Z* nuclei, and the bandhead excitation energies of odd-*Z* rare-earth nuclei at different quasiproton configurations. These characters provide useful information for understanding the band structure in odd-odd ^{170}Ta. In the framework of the standard cranked-shell model, the two-quasiparticle routhians $e'(\omega)$ of a odd-odd nucleus can be theoretically reproduced by summing the Routhians of the associated quasiproton and quasineutron. This simple additivity rule has been used here and the two-quasiparticle routhians have been predicted as shown in Fig. 9 for the rotational bands in ^{170}Ta under different quasiparticle configurations. In these calculations, the Harris parameters listed in Table II are used. The one-quasiparticle Routhian has been calculated using the data of ^{169,171}Ta [48,44] and ^{169,171}Hf [49,65], respectively. The bandhead excitation energies for the one-quasiparticle bands are taken from Refs. [53,66,67]. The sum of one-quasiparticle bandhead energies are used as the estimation of related two-quasiparticle bandhead energies. The Gallagher-Moszkowski splitting [62] and the rotational term [68] are neglected, their influences on the trends of two-quasiparticle Routhians are expected to be small in the high-frequency region. As clearly demonstrated in Fig. 9(c), two-quasiparticle routhians $e'(\omega)$ of ^{170}Ta can

TABLE II. Parameters used for calculation of $B(M1)/B(E2)$ ratios and alignments i_x for the rotational bands in ^{170}Ta and the associated odd-mass neighbors.

Nucleus	Configuration	K^π	J_0 ($\mathrm{MeV}^{-1}\hbar^2$)	J_1 ($\mathrm{MeV}^{-3}\hbar^4$)	i_x ($\hbar$)	$\hbar\omega_C$ (MeV)	g_n or g_p	g_R
^{168}Hf	yrast	0^+	23.9	174.4	0	0.265(5)		
^{170}Hf	yrast	0^+	28.7	218.7	0	0.265(5)		
^{169}Hf	$\nu 5/2^+[642]$	$5/2^+$	32.6	102.8	4.1	0.315(5)	−0.33	0.14
^{169}Hf	$\nu 5/2^-[523]$	$5/2^-$	37.2	197.9	0.7	0.240(5)	0.25	0.27
^{171}Hf	$\nu 5/2^-[512]$	$5/2^-$	28.7	218.7	1.2	0.240(5)	−0.49	0.28
^{169}Ta	$\pi 1/2^-[541]$	$1/2^-$	33.3	51.6	2.2	0.305(5)	0.74	0.4
^{169}Ta	$\pi 9/2^-[514]$	$9/2^-$	23.0	181.5	1.8	0.24	1.24	0.4
^{169}Ta	$\pi 5/2^+[402]$	$5/2^+$	21.0	249.1	0.7	0.24	1.59	0.49
^{171}Ta	$\pi 7/2^+[404]$	$7/2^+$	28.7	218.7	1.2	0.24	0.73	0.312
^{170}Ta *A*	$\pi 9/2^-[514]\otimes \nu i_{13/2}$	7^-	28.1	143.5	5.8	$\geqslant$0.29		0.248
^{170}Ta *B*	$\pi 1/2^-[541]\otimes \nu i_{13/2}$	2^-,3^-	31.4	89.9	6.2	$>$0.34		0.248
^{170}Ta *C*	$\pi 5/2^+[402]\otimes \nu i_{13/2}$	5^+	26.6	200.6	4.8	0.29(1)		0.338
^{170}Ta	$\pi 7/2^+[404]\otimes \nu i_{13/2}$	6^+						0.158
^{170}Ta	$\pi 1/2^-[541]\otimes \nu 5/2^-[523]$	3^+						0.378

be separated into two groups. The lower-lying group, which is expected to be favorably populated, corresponds to the configurations of the $5/2^+[642]$ neutron coupled to the $1/2^-[541]$, $9/2^-[514]$, $5/2^+[402]$, and $7/2^+[404]$ protons, respectively. The other group is higher-lying and thus the associated rotational bands are expected to be less strongly populated. This theoretical estimation is used as an additional argument for the configuration assignment as discussed in the following. The experimental Routhians are also presented in Fig. 9(d) for comparisons.

A. Signature inversion in band *A*

Band *A* is the most strongly populated in the heavy-ion reaction used here and considered most likely to be the yrast band based on the $\pi 9/2^-[514](\alpha=\pm 1/2)\otimes \nu 5/2^+[642](\alpha=1/2)$ quasiparticle configuration. The configuration assignment is mainly based on previous studies of its neighboring odd-odd and odd-*A* nuclei in $A=160$ mass region. The proton $h_{11/2}$-$9/2^-[514]$ bands in ^{169}Ta and ^{171}Ta have been observed to be intensely populated in the heavy-ion induced fusion-evaporation reactions [44,48]. The low-*K* components of the $i_{13/2}$ neutron configuration are yrast in the odd-*N* nuclei in this mass region. As a result, the most probable configuration for this band must be a low-*K* $i_{13/2}$ neutron (mainly $5/2^+[642]$ component) coupled to the $9/2^-[514]$ proton. The two-quasiparticle Routhian for this configuration is predicted to be lower-lying as displayed in Fig. 9(c) indicating that this band should be strongly populated. The theoretical $B(M1)/B(E2)$ ratios have been calculated using Eqs. (3)–(6) and the parameters tabulated in Table II. The calculated results are compared with the experimental data in Fig. 8(a). The agreement is very good under the assumption of the $\pi 9/2^-[514]\otimes \nu 5/2^+[642]$ quasiparticle configuration.

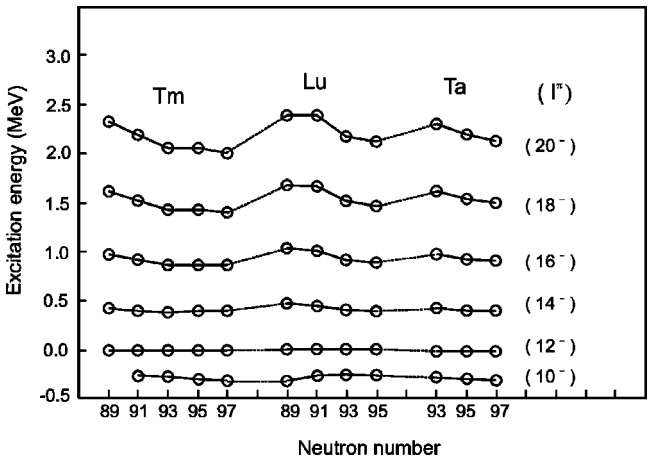

FIG. 6. Transition energy systematics for the $\alpha_f=0$ transition sequences of the $\pi h_{11/2}\otimes \nu i_{13/2}$ bands in $^{158-166}$Tm [10–21], $^{160-166}$Lu [22–31], and $^{166-170}$Ta [31–33] nuclei. (12^-) levels are taken as a reference.

Previous studies of odd-odd nuclei in this mass region have established a consistent pattern of the energy signature dependence. Systematic studies and analysis have been made in several recent publications [8,26,27,31,69,70], the main features can be outlined as follows:

(1) The energy signature inversion occurs at low rotational frequencies in all the $\pi h_{11/2}\otimes \nu i_{13/2}$ bands of odd-odd nuclei in the $65\leqslant Z\leqslant 73$, $89\leqslant N\leqslant 97$ region.

(2) For a chain of isotopes, the anomalous splitting amplitude decreases with increasing the neutron number.

(3) For a chain of isotones (such as $N=91$), with the increase of proton number, the splitting amplitude changes first from larger (^{156}Tb) to smaller (^{158}Ho) and then to the larger amplitude again (^{160}Tm and ^{162}Lu).

(4) Up to a certain spin, signature splitting recovers to be normal. Associated with this crossing point, the so-called

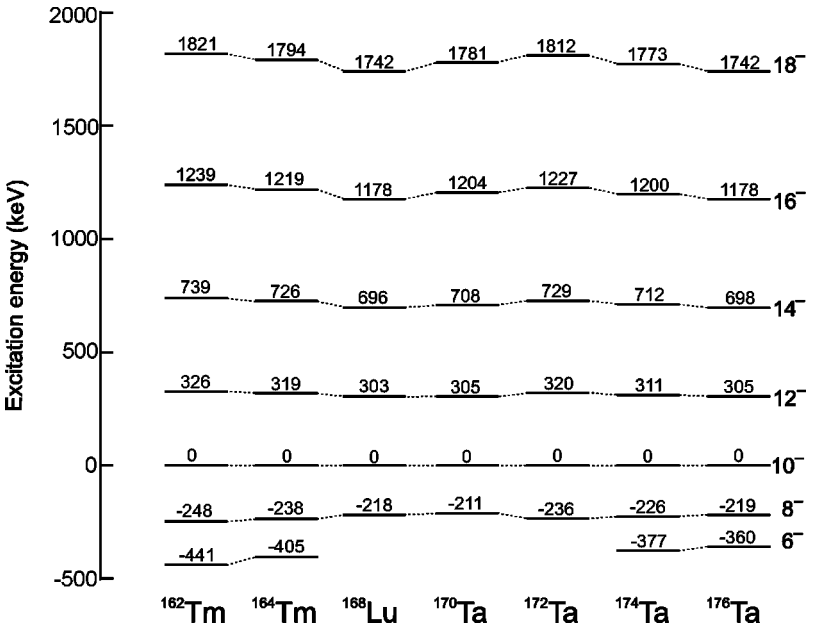

FIG. 7. Transition energy systematics for the semidecoupled bands in ^{170}Ta (present work), ^{172}Ta [56,57], ^{174}Ta [42], ^{176}Ta [55], ^{168}Lu [54], and ^{162,164}Tm [42].

signature crossing frequency can be extracted, and it changes regularly with Z and N. For a fixed $N-Z$ value, the inversion frequencies remain approximately constant.

The signature dependence of a rotational band is related to the K quantum number of associated single-particle states, and the deformation of the nucleus. In band A, the energy signature splitting is small compared with that of its neighboring odd-mass nuclei. In order to illustrate this small signature splitting, an energy difference $\Delta E(I)$ defined as

$$\Delta E(I)=[E(I)-E(I-1)]-\tfrac{1}{2}[E(I+1) -E(I)+E(I-1)-E(I-2)] \quad (8)$$

is plotted as a function of spin for the similar bands in ^{166,168,170}Ta in Fig. 10. Here $E(I)$ is the level energy of state I, $\Delta E(I)$ is directly proportional to the energy difference of the two signatures, but magnified by approximately a factor of 2 [29].

It is clearly shown in this figure that the energy signature inversion in the $\pi h_{11/2}\otimes \nu i_{13/2}$ band of ^{170}Ta has been observed below $I=17\hbar$, above this point the signature splitting becomes normal. The three bands in ^{166,168,170}Ta have a similar trend indicating that the same quasiparticle configuration of $\pi h_{11/2}\otimes \nu i_{13/2}$ is involved. The amplitude of anomalous signature splitting in Ta is larger than that in its lower Z isotones, and it decreases with the neutron number. From the signature crossing point of $I=17\hbar$, the inversion frequency is extracted to be $\hbar\omega=0.27(1)$ MeV, this value is very close to that [8,27,69] of similar bands in $N-Z=24$ nuclei of ^{154}Tb ($\hbar\omega=0.28$ MeV), ^{158}Ho ($\hbar\omega=0.25$ MeV), ^{162}Tm ($\hbar\omega=0.26$ MeV), and ^{166}Lu ($\hbar\omega=0.26$ MeV). All these properties are in good agreement with the systematics (1)–(4) as mentioned above.

Different mechanisms have been proposed to interpret this signature inversion phenomenon using several theoretical approaches [34–41], and some comments on these explanations are given in Refs. [28,69]. We would like to address

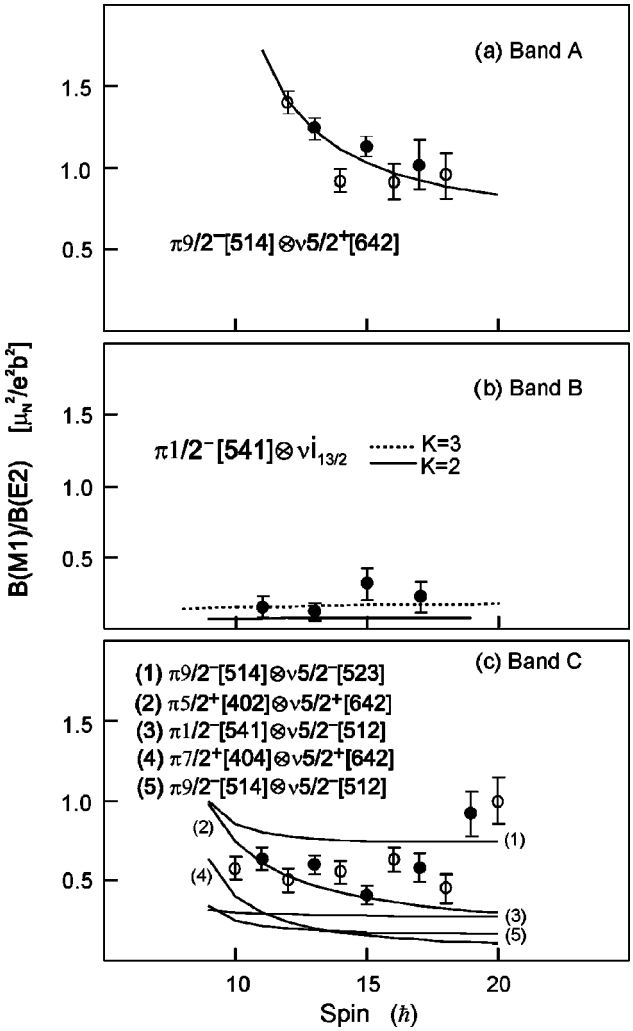

FIG. 8. Experimental $B(M1)/B(E2)$ ratios as a function of spin for (a) band A, (b) band B, and (c) band C. The curves correspond to calculations based on the geometric model of Donau and Frauendorf [58].

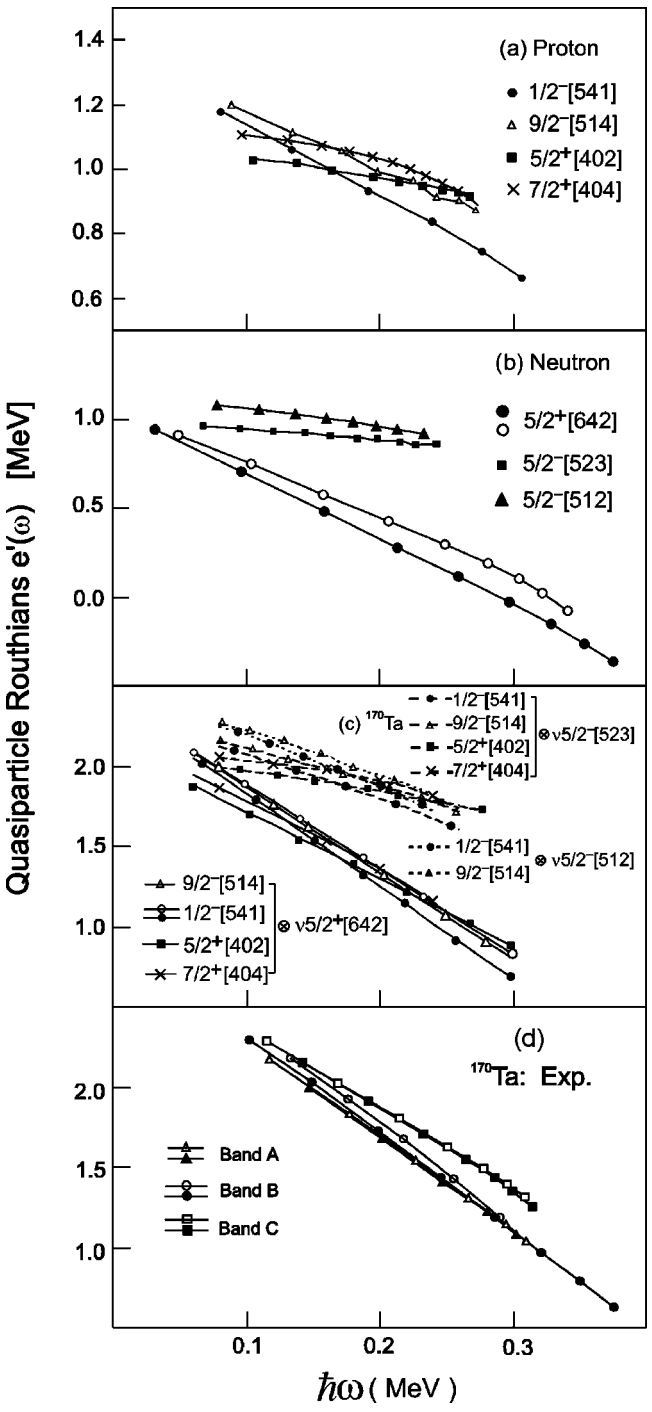

FIG. 9. The predicted two-quasiparticle routhians for (c) ^{170}Ta as a function of rotational frequency $\hbar\omega$ obtained by summing the one-quasiparticle Routhians of the corresponding (a) proton and (b) neutron. The experimental Routhians for ^{170}Ta are shown in (d) for comparisons, an average excitation energy of 0.8 MeV is used for the lowest levels of each band.

that the signature inversion presents in a wider nuclear range than previously predicted [34] and the particular shell filling seems not to be a strict restriction to the presence of this phenomenon.

B. Level staggering in Band *B*

Band *B* is supposed to be the semidecoupled band based on $\pi 1/2^-[541](\alpha=1/2)\otimes\nu i_{13/2}(\alpha=\pm 1/2)$-$5/2^+[642]$ quasiparticle configuration. This assignment is suggested according to the following considerations: (1) The theoretical calculations based on cranked shell model predict that the two-quasiparticle routhian for this configuration is lower-lying as displayed in Fig. 9(c) and should be strongly populated in the reaction used here. (2) The large energy signature splitting is observed at lower rotational frequencies. In this region, only the $\pi 1/2^-[541]$ or $\nu 5/2^+[642]$ one-quasiparticle bands have such a large signature splitting. The signature splitting of $\pi 1/2^-[541]$ bands is much larger than that of $\nu 5/2^+[642]$ bands, and therefore the signature splitting originates most probably from the contribution of the $i_{13/2}$ neutron (mainly the $5/2^+[642]$ component). (3) The band crossing frequency ($\hbar\omega_C \geqslant 0.34$ MeV) is much delayed in comparison with $\hbar\omega_C$ values of its neighboring even-even and odd-*A* nuclei. This delay is clearly demonstrated in Fig. 5 and Fig. 12(a) where both alignment i_x and dynamic moment of inertia $J^{(2)}$ have a sudden increase around $\hbar\omega_C = 0.29$ MeV for bands *A* and *C* but not for band *B*. (4) The experimental $B(M1)/B(E2)$ ratio for band *B* is smallest and can be roughly reproduced [see Fig. 8(b)] theoretically under the assumption of $\pi 1/2^-[541](\alpha=1/2)\otimes\nu i_{13/2}(\alpha=\pm 1/2)$-$5/2^+[642]$ quasiparticle configuration.

Recently, the firm spin assignments for the semidecoupled bands in ^{162,164}Tm and ^{174}Ta [42] have been made through a spectroscopic method. As a consequence, the low-spin signature inversion has been identified in the $\pi 1/2^-[541]\otimes\nu i_{13/2}$ structure. It is, therefore, a natural extrapolation (or interpolation) that the low-spin signature inversion should occur in similar bands of lighter Ta and Lu isotopes such as in ^{170,172}Ta and $^{166-170}$Lu. Indeed, a systematic analysis has been made in a recent literature [57] in which the low-spin signature inversion has been suggested for the semidecoupled bands in ^{176,178}Re, ^{172,176}Ta, and ^{170}Lu. We plot the energy staggering defined as $E(I)-E(I-1)$ versus spin *I* in Fig. 11 for the semidecoupled bands in ^{170}Ta and those in some neighboring nuclei. The high-spin data of ^{168}Lu are from [54,71]. We accept the spins used in [57] for ^{172}Ta which is arbitrarily increased by $3\hbar$ with respect to the previous assignment [56]. The similarity of the staggering pattern is impressive. First, the signature splitting is inverted at lower spins for all the semidecoupled bands shown in this figure; the levels with a favored signature ($\alpha^f_{p-n}=\alpha^f_p+\alpha^f_n=1/2+1/2=1$) are lying higher than the levels with an unfavored signature ($\alpha^{uf}_{p-n}=\alpha^f_p+\alpha^{uf}_n=1/2-1/2=0$). Second, the signature splitting reverts (or tend to revert) to the normal ordering at a certain high-spin value. The reversion points have been observed (see Fig. 11) in ^{162,164}Tm, ^{168}Lu [71], ^{174}Ta, and ^{176}Re, respectively. (The reversion points in ^{170}Lu and ^{172}Ta were also reported in [57].) Although the reversion point is not reached in ^{170}Ta because of the lack of higher spin data, the tendency towards reversion at about $I=(20)\hbar$ is evident as shown in Fig. 11. For most of the

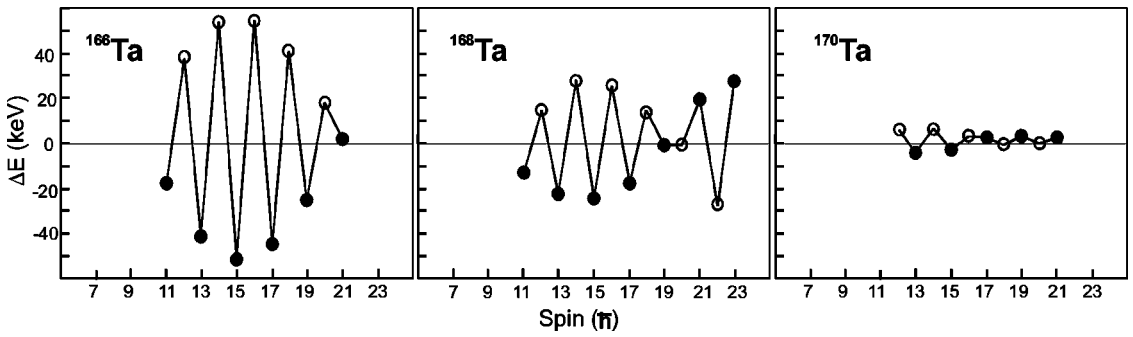

FIG. 10. Energy signature splitting, $\Delta E(I)$ defined as Eq. (8), as a function of spin for the $\pi h_{11/2}\otimes\nu i_{13/2}$ bands in ^{166,168}Ta [31–33] and ^{170}Ta (present work). The open circles represent the $\Delta I=2$ transition sequence with favored signature $\alpha_f=0$, the filled circles for the unfavored one $\alpha_{uf}=1$.

semidecoupled bands in this mass region, the spin assignments based on spectroscopic methods are rather difficult. According to our experiences, an uncertainty of $2\hbar$ may be introduced relying on the systematics of level spacings and the additivity rule for alignment, thus the observation of reversion point becomes very important and could be regarded as an indirect evidence of low-spin signature inversion. For a chain of isotopes, the reversion spin seems to decrease with decreasing the neutron number (see Fig. 11 and [57]). It is thus expected that the reversion points could be observed at moderate high spins in ^{166}Lu, ^{168,170}Ta and ^{174}Re.

C. Band *C*

Band *C* is newly found in this work, and it shows the strongly coupled characters with small signature splitting. In order to identify the quasiparticle configuration, the alignment $i_x(\omega)$ and the dynamic moment of inertia $J^{(2)}(\omega)$, as a function of rotational frequency have been analyzed both for this band and the low-lying one-quasiparticle bands in the neighboring odd mass nuclei. The band crossing frequencies have been extracted and tabulated in Table II using the method described and applied in [56,72,73]. As shown in Figs. 5 and 12, band *C* has a similar trend as band *A*, and a sudden increase occurs at about $\hbar\omega_C\approx 0.29$ MeV. This frequency is delayed in comparison with neutron *AB* crossing in the neighboring even-even nuclei (*AB* crossing frequency in ^{168}Hf and ^{170}Hf is 0.265 MeV as presented in Table II). In this mass region, the one-quasiparticle bands based on $\pi 1/2^-[541]$ and $\nu i_{13/2}$ configurations are known to have a relatively large crossing frequency. Therefore, one of these particular orbitals must be involved in band *C*. Apart from the already known configurations for bands *A* and *B*, the couplings of $\pi 5/2^+[402]\otimes\nu 5/2^+[642]$, $\pi 7/2^+[404]\otimes\nu 5/2^+[642]$, $\pi 1/2^-[541]\otimes\nu 5/2^-[523]$, and $\pi 1/2^-[541]\otimes\nu 5/2^-[512]$ are expected to be the most probable candidates for this band.

The $B(M1)/B(E2)$ ratios for this band have been calculated using Eqs. (3)–(6) under the assumption of the four configurations cited above. The calculated results have been plotted in Fig. 8(c). The parameters in Table II are used for

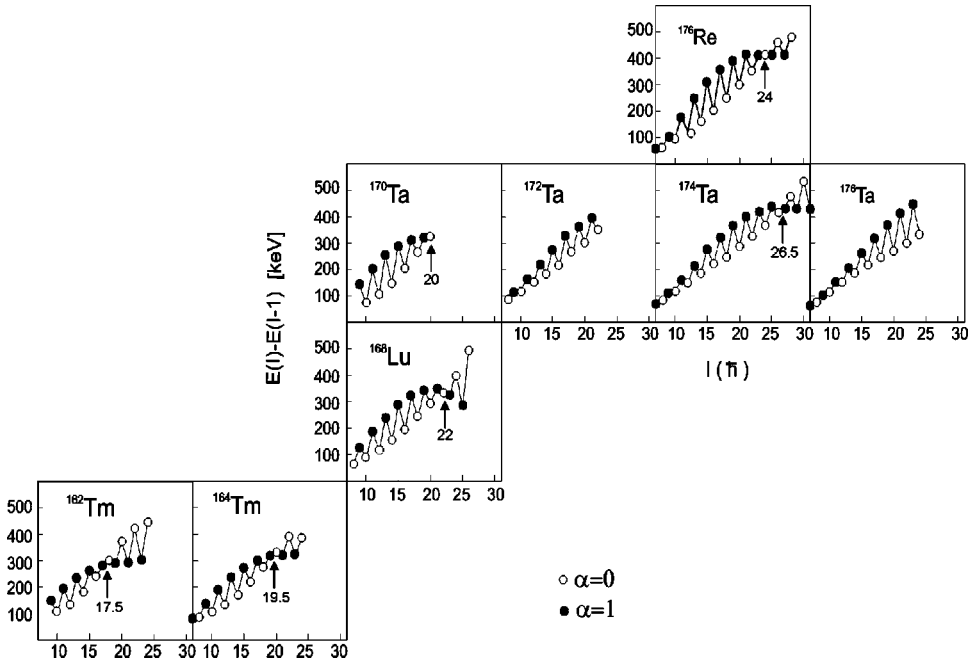

FIG. 11. Level staggering for the semidecoupled bands in ^{176}Re [57], ^{170}Ta (present work), $^{172-176}$Ta [56,57,42,55], ^{168}Lu [54,71], and ^{162,164}Tm [42]. The filled circles represent the $\Delta I=2$ transition sequence with signature $\alpha_f=1$, the open circles for the unfavored one $\alpha_{uf}=0$.

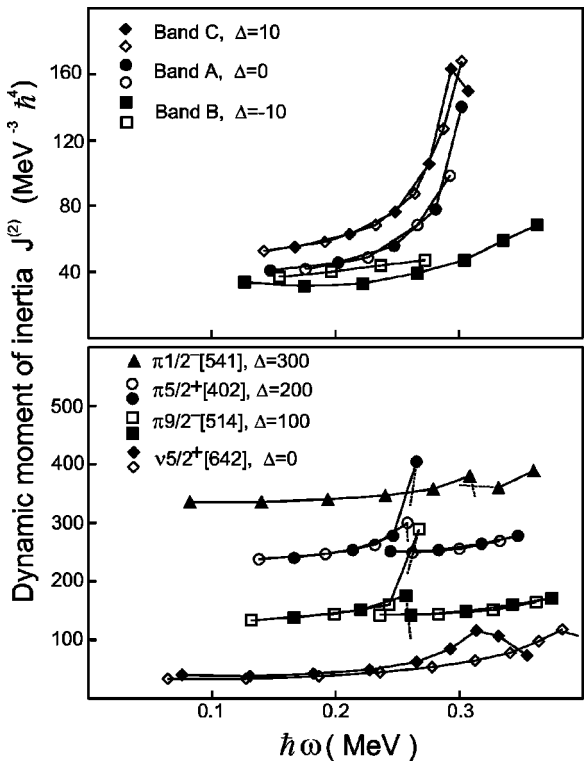

FIG. 12. Plot of dynamic moment of inertia $J^{(2)}$ as a function of rotational frequencies for the three bands of ^{170}Ta and the related one-quasiparticle bands in ^{169}Ta [48] and ^{169}Hf [49]. Each curve is shifted by adding a Δ for clear illustration. The dotted line indicates a sharp discontinuity (decrease) at that point.

theoretical calculations. As is clear in Fig. 8(c), the experimental ratios below $I=18\hbar$ are closer to those calculated for the $\pi 5/2^+[402]\otimes\nu 5/2^+[642]$ configuration. We have noticed the delayed *AB* crossing frequencies recently observed in the $\pi h_{11/2}\otimes\nu h_{9/2}$ bands of ^{160}Tm [16] and ^{164}Lu [28,29], and the corresponding one-quasiparticle $\pi 9/2^-[514]$ and $\nu 5/2^-[512]$ bands have also been identified in ^{169,171}Ta [48,44] and ^{171}Hf [65], therefore, $B(M1)/B(E2)$ ratios for the $\pi 9/2^-[514]\otimes\nu 5/2^-[512]$ coupling are also calculated and shown in Fig. 8(c). However, the agreement with experimental values is poor compared with the result of the $\pi 5/2^+[402]\otimes\nu 5/2^+[642]$ coupling. The calculated quasiparticle Routhian based on CSM is lower-lying [see Fig. 9(c)] for this two-quasiparticle configuration. These arguments support the configuration assignment of $\pi 5/2^+[402]\otimes\nu 5/2^+[642]$ for band *C*.

D. Band crossing frequencies

If the configuration assignment mentioned above is accepted, the upbend or backbend of these bands should correspond to the neutron *BC* or *AD* crossing. Figure 12 shows the plot of dynamic moment of inertia $J^{(2)}$, defined as $J^{(2)}(I)=4/\Delta E_\gamma(I)$, versus the rotational frequencies for the three bands in ^{170}Ta and the related one-quasiparticle bands in ^{169}Ta and ^{169}Hf; this quantity can be calculated directly from observed γ ray energies, $E_\gamma(I)$, and differences of γ-ray energy between neighboring transitions, $\Delta E_\gamma(I)=E_\gamma(I+2)-E_\gamma(I)$, respectively. To make a clear illustration, each curve is shifted by adding a Δ as indicated in the figure, and the dotted line indicates a sharp discontinuity (decrease) at that point. It is clearly demonstrated in Figs. 5 and 12 that there is a sudden increase for bands *A* and *C* both in alignment i_x (Fig. 5) and in the dynamic moment of inertia $J^{(2)}$ (Fig. 12). This sudden increase disappears in band *B*. The band crossing frequency can be extracted from the intersection of two slopes in the routhians $e'(\omega)$ versus $\hbar\omega$ plots before and after the first backbend [72]. Although the level scheme given in Fig. 3 cannot be extended to higher spins, the band crossing frequencies could still be read out as $\hbar\omega_C\geqslant 0.34$ MeV for band *B*, and $\hbar\omega_C=0.29(1)$ MeV for band *C*, respectively. From systematic inspection of Table II, the statement can be concluded: the first band crossing frequency for the $\pi 1/2^-[541]\otimes\nu 5/2^+[642]$ ($\pi 5/2^+[402]\otimes\nu 5/2^+[642]$) band is larger (smaller) than the *BC* crossing frequency of the $\nu i_{13/2}$ bands in its neighboring odd-*N* nuclei. A similar experimental result has also been observed in the rotational bands of ^{172}Ta [56,73].

The configuration-dependent band crossing frequency could be understood when associated with the similar phenomenon discovered in the neighboring odd-*Z* nuclei. The *AB* crossing frequencies for the $\pi 9/2^-[514]$, $\pi 5/2^+[402]$ bands in Lu and Ta isotopes are very close to, but slightly lower (roughly 20 keV lower) than those in the yrast sequences of their even-even neighbors [48,51]. However, in contrast to these cases, a significant delay (varied from 30 to 75 keV) in the *AB* crossing frequencies has been observed in the $\pi 1/2^-[541]$ bands ([74], and references therein). This phenomenon has been extensively studied and attributed to the shape-driving effect [64,75,76], residual proton-neutron interactions [77], quadrupole pairing [78], and decoupling term [79], respectively. The study of this subject is out of the scope of this paper, we would like to point out that the mechanism, leading to the configuration-dependent *AB* crossing, exists in the odd-odd nuclei and has been exhibited in the first band crossing frequencies. For instance, the $\nu 5/2^+[642]$ band in ^{169}Hf [49] backbends at $\hbar\omega_C=0.315$ MeV, 50 keV delayed with respect to its even-even core ^{168}Hf of $\hbar\omega_C=0.265$ MeV (see Table II). The delay of the *AB* band crossing frequency for the $1/2^-[541]$ band in ^{169}Ta [48] is 40 keV. Thus the first band crossing in the semidecoupled band of ^{170}Ta will be delayed as high as 90 keV due to the contributions of both quasiproton and quasineutron. Similarly, taking the *AB* crossing frequency as $\hbar\omega_C=0.24$ MeV [48] for the $\pi 5/2^+[402]$ and $\pi 9/2^-[514]$ bands, the crossing frequencies for the bands based on $\pi 9/2^+[514]\otimes\nu 5/2^+[642]$ (band *A*) and $\pi 5/2^+[402]\otimes\nu 5/2^+[642]$ (band *C*) can be predicted to be $\hbar\omega_C=0.29$ MeV using the additivity effect for the crossing frequency shifts [73]. Experimentally a sudden increase in $J^{(2)}$ and $i_x(\omega)$ has been observed at $\hbar\omega_C=0.29$ MeV for bands *A* and *C*. However, a smooth variation is found for band *B* up to the frequencies as high as 0.35 MeV. These observations are consistent with expectations cited above.

IV. SUMMARY AND CONCLUSIONS

To summarize, the high-spin states in ^{170}Ta have been further investigated by the in-beam spectroscopic methods.

A level scheme consisting of three rotational bands has been established. The quasiparticle configurations of these bands are suggested based on the existing knowledge of neighboring nuclei and the measured $B(M1)/B(E2)$ ratios as well as the properties in the framework of cranked-shell model. Apart from the $\pi 9/2^-[514]\otimes\nu 5/2^+[642]$ yrast band and the $\Delta I=2$ transition sequence in the semidecoupled band, a $\pi 5/2^+[402]\otimes\nu 5/2^+[642]$ strongly coupled band and a new $\Delta I=2$ transition sequence based on the $\pi 1/2^-[541]\otimes\nu 5/2^+[642]$ configuration have been identified in this work. The $\pi 9/2^-[514]\otimes\nu 5/2^+[642]$ yrast band exhibits an anomalous signature splitting at low rotational frequencies. The first band crossing frequency in the $\pi 1/2^-[541]\otimes\nu 5/2^+[642]$ band is much delayed with respect to the *BC* crossing in the neighboring $\nu i_{13/2}$ bands. A slightly smaller band crossing frequency [$\hbar\omega_C=0.29(1)$ MeV] is also observed in the $\pi 5/2^+[402]\otimes\nu 5/2^+[642]$ band with respect to the *BC* crossing ($\hbar\omega_C=0.315$ MeV) of neighboring odd-*N* nuclei. This configuration-dependent band crossing frequencies in ^{170}Ta have been discussed, and attributed qualitatively to the same mechanisms leading to the configuration-dependent *AB* crossing in the related bands of neighboring odd-*Z* isotopes. Low-spin signature inversion in the semidecoupled band of ^{170}Ta is suggested. Although well-behaved systematics could be presented both in the consecutive $E2$ transition energies and in the level staggering pattern among the similar bands of neighboring nuclei, the firm spin assignments are needed in order to confirm the low-spin signature inversion in the semidecoupled band of lighter odd-odd Ta.

ACKNOWLEDGMENTS

The authors wish to thank the staffs in the Accelerator division of IMP and CIAE for providing ^{16}O beam and Dr. X. Y. Wang for preparing the target. This work was partly supported by the State's Education Committee of China and the National Natural Science Foundation of China under Grant No. 19605008.

[1] J. A. Pinston, R. Bengtsson, E. Monnand, F. Schussler, and D. Barneoud, Nucl. Phys. **A361**, 464 (1981).
[2] R. Bengtsson, J. A. Pinston, D. Barneoud, E. Monnand, and F. Schussler, Nucl. Phys. **A389**, 158 (1982).
[3] G. Lovhoiden, Phys. Scr. **25**, 459 (1982).
[4] S. H. Bhatti, J. C. Kim, S. J. Chae, J. H. Ha, C. S. Lee, J. Y. Moon, C. B. Moon, T. Komatsubara, J. Lu, M. Matsuda, T. Hayakawa, T. Watanabe, and K. Furuno, Z. Phys. A **353**, 119 (1995).
[5] N. Rizk and J. Boutlet, J. Phys. (France) Lett. **37**, 197 (1976).
[6] J. R. Leigh, F. S. Stephens, and R. M. Diamond, Phys. Lett. **33B**, 410 (1970).
[7] J. A. Pinston, S. Andre, D. Barneoud, C. Foin, J. Genevey, and H. Frisk, Phys. Lett. **137B**, 47 (1984).
[8] S. Drissi, Z. Li, M. Deleze, J. Kern, and J. P. Vorlet, Nucl. Phys. **A600**, 63 (1996).
[9] J. L. Salicio, M. Deleze, S. Drissi, J. Kern, S. J. Mannanal, J. P. Vorlet, and I. Hamamoto, Nucl. Phys. **A512**, 109 (1990).
[10] S. Drissi, S. Andre, J. Genevey, V. Barci, A. Gizon, J. Gizon, J. A. Pinston, J. Jastrzebski, R. Kossakowski, and Z. Preobisz, Z. Phys. A **302**, 361 (1981).
[11] C. Foin, S. Andre, D. Barneoud, J. Genevey, J. A. Pinston, and J. Salicio, Phys. Lett. **159B**, 5 (1985).
[12] R. Holtzmann, M. Loiselet, M. A. Van Hove, and J. Vervier, Phys. Rev. C **31**, 421 (1985).
[13] S. Drissi, A. Bruder, J.-Cl. Dousse, V. Ionescu, J. Kern, J.-A. Pinston, S. Andre, D. Barneoud, J. Genevey, and H. Frisk, Nucl. Phys. **A451**, 311 (1986).
[14] S. Andre, D. Barneoud, C. Foin, J. Genevey, and J. C. Merdinger, Z. Phys. A **332**, 233 (1989).
[15] M. A. Reley, Y. A. Akovali, C. Baktash, M. L. Halbert, D. C. Hensley, N. R. Johnson, I. Y. Lee, F. K. McGowan, A. Virtanen, L. H. Courtney, V. P. Janzen, L. L. Riedinger, L. Chaturvedi, and J. Simpson, Phys. Rev. C **39**, 291 (1989).
[16] S. Andre, D. Barneoud, C. Foin, J. Genevey, J. A. Pinston, B. Haas, J. P. Vivien, and J. A. Kreiner, Z. Phys. A **333**, 233 (1989).
[17] S. Drissi, J.-Cl. Dousse, V. Ionescu, J. Kern, J.-A. Pinston, and D. Barneoud, Nucl. Phys. **A466**, 385 (1987).
[18] S. Elfstrom, I. Forsblom, K. Fransson, L. Hildingsson, and W. Klamra, Z. Phys. A **305**, 87 (1982).
[19] S. Drissi, A. Bruder, M. Carlen, J. Cl. Dousse, M. Gasser, J. Kern, S. J. Mannanal, B. Perny, Ch. Rheme, J. L. Salicio, J. P. Vorlet, and I. Hamamoto, Nucl. Phys. **A543**, 495 (1992).
[20] S. J. Mannanal, B. Boschung, M. W. Carlen, J. Cl. Dousse, S. Drissi, P. E. Garret, J. Kern, B. Perny, Ch. Rheme, J. P. Vorlet, C. Gunthe, J. Manns, and U. Muller, Nucl. Phys. **A582**, 141 (1995).
[21] S. Drissi, S. Andre, D. Barneoud, C. Foin, J. Genevey, and J. Kern, Nucl. Phys. **A601**, 234 (1996).
[22] H. B. Sun, Y. J. Ma, H. Zheng, Y. Z. Liu, C. X. Yang, S. X. Wen, G. J. Yuan, and G. S. Li, Z. Phys. A **351**, 241 (1995).
[23] Y. H. Zhang, X. H. Zhou, Z. Q. Zhao, X. F. Sun, X. G. Lei, Y. X. Guo, Z. Liu, X. F. Chen, Y. T. Zhu, S. X. Wen, G. J. Yuan, and X. A. Liu, Chin. J. Nucl. Phys. **17**, 250 (1995); Z. Phys. A **355**, 335 (1996).
[24] S. G. Zhou, Y. Z. Liu, Y. J. Ma, and C. X. Yang, J. Phys. G **22**, 415 (1996).
[25] M. A. Cardona, M. E. Debray, D. Hojman, A. J. Kreiner, H. Somacal, J. Davidson, M. Davidson, D. De Acuna, D. R. Napoli, J. Rico, D. Bazzacco, R. Burch, S. M. Lenzi, C. R. Alvarez, N. Blasi, and G. L. Bianco, Z. Phys. A **354**, 5 (1996).
[26] M. A. Cardona, J. Davidson, D. Hojman, M. E. Debray, A. J. Kreiner, H. Somacal, M. Davidson, D. R. Napoli, D. Bazzacco, N. Blasi, R. Burch, D. De Acuna, S. M. Lenzi, G. L. Bianco, J. Rico, and C. R. Alvarez, Phys. Rev. C **56**, 707 (1997).
[27] S. L. Gupta, S. C. Pancholi, P. Juneja, D. Mehta, A. Kumar, R. K. Bhowmik, S. Muralithar, G. Rodrigues, and R. P. Singh, Phys. Rev. C **56**, 1281 (1997).
[28] P. Juneja, S. L. Gupta, S. C. Pancholi, D. Mehta, A. Kumar, D.

Mehta, L. Chaturvedi, S. K. Katoch, S. Malik, G. Shanker, R. K. Bhowmik, S. Muralithar, G. Rodrigues, and R. P. Singh, Phys. Rev. C **53**, 1221 (1996).

[29] X. H. Wang, C. H. Yu, D. M. Cullen, D. C. Bryan, M. Devlin, M. J. Fitch, A. Galindo-Uribarri, R. W. Gray, D. M. Herrick, R. W. Ibbotson, K. L. Kurz, S. Mullins, S. Pilotte, D. C. Radfold, M. R. Satteson, M. W. Simon, D. Ward, C. Y. Wu, and L. H. Yao, Nucl. Phys. **A608**, 77 (1997).

[30] D. Hojman, A. J. Kreiner, M. Davidson, J. Davidson, M. Debray, E. W. Cybulska, P. Pascholati, and W. A. Seale, Phys. Rev. C **45**, 90 (1992).

[31] Y. Z. Liu, Y. J. Ma, H. T. Yang, and S. G. Zhou, Phys. Rev. C **52**, 2514 (1995).

[32] H. Zheng, Y. Z. Liu, Y. J. Ma, H. B. Sun, S. G. Zhou, H. T. Yang, J. D. Hou, X. A. Liu, Z. Y. Dai, X. G. Wu, S. X. Wen, G. J. Yuan, and C. X. Yang, J. Phys. G **23**, 723 (1997).

[33] K. Theine, C. X. Yang, A. P. Byrne, H. Hubel, R. Chapman, D. Clarke, F. Khazaie, J. C. Lisle, J. N. Mo, J. D. Garrett, and H. Ryde, Nucl. Phys. **A536**, 418 (1992).

[34] R. Bengtsson, H. Frisk, R. F. May, and J. A. Pinston, Nucl. Phys. **A415**, 189 (1984).

[35] M. Matsuzaki, Phys. Lett. B **269**, 23 (1991).

[36] I. Hamamoto, Phys. Lett. B **235**, 221 (1990).

[37] A. K. Jain and A. Goel, Phys. Lett. B **277**, 233 (1992).

[38] R. R. Zheng, S. Q. Zhu, and Y. W. Pu, Phys. Rev. C **56**, 175 (1997).

[39] K. Hara and Y. Sun, Nucl. Phys. **A531**, 221 (1991).

[40] K. Hara, Nucl. Phys. **A557**, 449c (1993).

[41] N. Yoshida, H. Sagawa, and J. Otsuka, Nucl. Phys. **A567**, 17 (1994).

[42] R. A. Bark, J. M. Espino, W. Reviol, P. B. Semmes, H. Carlsson, I. G. Bearden, G. B. Hagemann, H. J. Jensen, I. Ragnarsson, L. L. Riedinger, H. Ryde, and P. O. Tjom, Phys. Lett. B **406**, 193 (1997).

[43] S. K. Katoch, S. L. Gupta, S. C. Pancholi, D. Mehta, S. Malik, G. Shanker, L. Chaturvedi, and R. K. Bhowmik, Z. Phys. A **358**, 5 (1997).

[44] J. C. Bacelar, R. Chapman, J. R. Leslie, J. C. Lisle, J. N. Mo, E. Paul, A. Simcock, J. C. Willmott, J. D. Garrett, G. B. Hagemann, B. Herskind, A. Holm, and P. M. Walker, Nucl. Phys. **A442**, 547 (1985).

[45] Y. H. Zhang, Q. Z. Zhao, X. H. Zhou, H. S. Xu, Y. X. Guo, X. G. Lei, J. Lu, S. F. Zhu, Q. B. Gou, H. J. Jin, Z. Liu, Y. X. Luo, X. F. Sun, and Y. T. Zhu, Chin. Phys. Lett. **14**, 409 (1997).

[46] Y. H. Zhang, S. Q. Zhang, Q. Z. Zhao, S. F. Zhu, H. S. Xu, X. H. Zhou, Y. X. Guo, X. G. Lei, J. Lu, Q. B. Gou, H. J. Jin, Z. Liu, Y. X. Luo, X. F. Sun, Y. T. Zhu, X. G. Wu, S. X. Wen, and C. X. Yang, Eur. Phys. J. A **1**, 119 (1998).

[47] X. G. Lei, Y. X. Guo, X. F. Sun, Z. Y. Sun, Z. G. Gan, X. H. Zhou, Z. Liu, and Y. X. Luo, Nucl. Electron. Detection Technol. **17**, 420 (1997) (in Chinese).

[48] S. G. Li, S. Wen, G. J. Yuan, G. S. Li, P. F. Hua, L. K. Zhang, Z. K. Yu, P. S. Yu, P. K. Weng, C. X. Yang, R. Chapman, D. Clarke, F. Khazaie, J. C. Lisle, J. N. Mo, J. D. Garrett, G. B. Hagemann, B. Herskind, and H. Ryde, Nucl. Phys. **A555**, 435 (1993).

[49] W. B. Gao, I. Y. Lee, C. Baktash, R. Wyss, J. H. Hamilton, C. M. Steele, C. H. Yu, N. R. Johnson, and F. K. McGowan, Phys. Rev. C **44**, 1380 (1991).

[50] J. C. Lisle, J. D. Garrett, G. B. Hagemann, B. Herskind, and S. Ogaza, Nucl. Phys. **A366**, 281 (1981).

[51] C.-H. Yu, G. B. Hagemann, J. M. Espino, K. Furuno, J. D. Garrett, R. Chapman, D. Clarke, F. Khazaie, J. C. Lisle, J. N. Mo, M. Bergstrom, L. Carlen, P. Ekstrom, J. Lyttkens, and H. Ryde, Nucl. Phys. **A511**, 157 (1990).

[52] Coral M. Baglin, Nucl. Data Sheets **77**, 125 (1996).

[53] F. Meissner, W. D. Schmidt-Ott, V. Frestein, T. Hild, E. Runte, H. Salewski, and R. Michaelsen, Z. Phys. A **337**, 45 (1990).

[54] S. K. Katoch, S. L. Gupta, S. C. Pancholi, D. Mehta, S. Malik, G. Shanker, L. Chaturvedi, and R. K. Bhowmik, Eur. Phys. J. A **4**, 307 (1999).

[55] F. G. Kondef, G. D. Dracoulis, A. P. Byrne, and T. Kibedi, Nucl. Phys. **A632**, 473 (1998).

[56] A. J. Kreiner, D. Hojman, J. Davidson, M. Davidson, M. Debray, G. Falcone, D. Santos, C. W. Beausang, D. B. Fossan, R. Ma, E. S. Paul, S. Shi, and N. Xu, Phys. Lett. B **215**, 629 (1988).

[57] M. A. Cardana, A. J. Kreiner, D. Hojman, G. Levinton, M. E. Debray, M. Davidson, J. Davidson, R. Pirchio, H. Somacal, D. R. Napoli, D. Bazzacco, N. Blasi, R. Burch, D. De Acuna, S. M. Lenzi, G. Lo Bianco, J. Rico, and C. Rossi Alvarez, Phys. Rev. C **59**, 1298 (1999).

[58] F. Donau, Nucl. Phys. **A471**, 469 (1987); F. Donau and S. Frauendorf, *Proceedings of the Conference on High Angular Momentum Properties of Nuclei*, Oak Ridge, Tennessee, 1982, edited by N. R. Johnson (Harwood Academic, Chur, Switzerland, 1982), p. 143.

[59] J. Kern and G. L. Struble, Nucl. Phys. **A286**, 371 (1977).

[60] F. Boehm, G. Goldring, G. B. Hagemann, G. D. Symons, and A. Tveter, Phys. Lett. **22**, 627 (1966).

[61] P. Raghavan, At. Data Nucl. Data Tables **42**, 189 (1989).

[62] C. J. Gallagher and S. A. Moszkowski, Phys. Rev. **111**, 1282 (1958).

[63] R. E. Leber, P. E. Haustein, and I.-M. Ladenbauer-Bellis, J. Inorg. Nucl. Chem. **38**, 951 (1976).

[64] W. Nazarewicz, M. A. Riley, and J. D. Garrett, Nucl. Phys. **A512**, 61 (1990).

[65] G. D. Dracoulis and P. M. Walker, Nucl. Phys. **A330**, 186 (1979).

[66] Y. H. Zhang, Q. Z. Zhao, S. F. Zhu, H. S. Xu, X. H. Zhou, Y. X. Guo, X. G. Lei, J. Lu, Q. B. Gou, H. J. Jin, Z. Liu, Y. X. Luo, X. F. Sun, and Y. T. Zhu, Eur. Phys. J. A **1**, 1 (1998).

[67] A. K. Jain, R. K. Sheline, P. C. Sood, and Kiran Jain, Rev. Mod. Phys. **62**, 393 (1990).

[68] R. W. Hoff, J. Kern, R. Piepenbring, and J. P. Boisson, *Proceedings of the Fifth International Symposium on capture gamma-ray spectroscopy and related topics*, Knoxville, Tennessee 1984, edited by S. Raman, AIP Conf. Proc. 152 (AIP, New York, 1985), pp. 274–289.

[69] Y. H. Zhang, X. H. Zhou, Z. Q. Zhao, X. F. Sun, X. G. Lei, Y. X. Guo, Z. Liu, X. F. Chen, Y. T. Zhu, S. X. Wen, G. J. Yuan, and X. A. Liu, High Energy Phys. Nucl. Phys. **21**, 15 (1997).

[70] T. Komatsubara, K. Furuno, T. Hosoda, J. Mukai, T. Hayakawa, T. Morikawa, Y. Iwata, N. Kato, J. Espino, J. Gascon, N. Gjorup, G. B. Hagemann, H. J. Jensen, D. Jerrestam, J.

Nyberg, G. Sletten, B. Cederwall, and P. O. Tjom, Nucl. Phys. **A557**, 419c (1993).
[71] S. Wen (unpublished).
[72] R. Bengtsson and S. Frauendorf, Nucl. Phys. **A327**, 139 (1979).
[73] A. J. Kreiner, Nucl. Phys. **A520**, 225c (1990).
[74] H. J. Jensen, R. A. Bark, R. Bengtsson, G. B. Hagemann, P. O. Tjom, S. Y. Araddad, C. W. Beausang, R. Chapman, J. Copnell, A. Fitzpatrick, S. J. Freeman, S. Leoni, J. C. Lisle, J. Simpson, A. G. Smith, D. M. Thompson, S. J. Warburton, and J. Wrzesinski, Z. Phys. A **358**, 5 (1997).
[75] H. J. Jensen, G. B. Hagemann, P. O. Tjom, S. Frauendorf, A. Atac, M. Bergstrom, A. Bracco, A. Brockstedt, H. Carlsson, P. Ekstrom, J. M. Espino, B. Herskind, F. Ingebretsen, J. Jongman, S. Leoni, R. M. Lieder, T. Lonnroth, A. Maj, B. Million, A. Nordlund, J. Nyberg, M. Piiparinen, H. Ryde, M. Sugawara, and A. Virtannen, Z. Phys. A **340**, 351 (1991).
[76] C. X. Yang, S. Wen, S. G. Li, G. J. Yuan, P. K. Weng, and G. S. Li, Chin. J. Nucl. Phys. **16**, 223 (1994).
[77] W. Satula, R. Wyss, and F. Donau, Nucl. Phys. **A565**, 573 (1993).
[78] Y. Sun, S. Wen, and D. H. Feng, Phys. Rev. Lett. **72**, 3483 (1994).
[79] C. S. Wu, Phys. Rev. C **51**, 1819 (1995).